An Efficiency-Optimal Control Method for Mono-Inverter Dual-PMSM Systems

Tianyi Liu, Maurice Fadel

This article has been accepted for publication in a future issue of this journal, but has not been fully edited. Content may change prior to final publication. Citation information: DOI 10.1109/TIA.2017.2768535, IEEE Transactions on Industry Applications

An Efficiency-Optimal Control Method for Mono-Inverter Dual-PMSM Systems

Tianyi LIU
Université de Toulouse; INPT; UPS; LAPLACE
(Laboratoire Plasma et Conversion d'Energie);
LAPLACE, 2 rue Charles Camichel, BP 7122
31071 Toulouse cedex 7, France.
tianyi.liu@laplace.univ-tlse.fr

Maurice FADEL
Université de Toulouse; INPT; UPS; LAPLACE
(Laboratoire Plasma et Conversion d'Energie);
LAPLACE, 2 rue Charles Camichel, BP 7122
31071 Toulouse cedex 7, France.
maurice.fadel@laplace.univ-tlse.fr

***Abstract*— Current research and development programs in aviation are promoting new technological advances to make electrical systems cheaper, lighter and more reliable. Mono-Inverter Dual-Permanent Magnet Synchronous Motor (MIDPMSM) systems tend to share the static converters in electro-mechanical systems by connecting motors in parallel. However several studies have shown that the efficiency of this configuration is lower than those with a traditional Mono-Inverter Mono-PMSM configuration, especially when unequal load torques are applied. In this paper, we propose an efficiency-optimized control method for MIDPMSM systems which has been designed using rigorous, mathematical calculations. The determinacy, stability, and optimal efficiency of the system, which are essential in an aviation application, are explained in detail. This new control structure is simple making current single PMSM systems easy to upgrade to support the MIDPMSM system. The experiment has demonstrated not only feasibility, but also significant improvements in performance.**

***Index Terms*— Dual-Permanent Magnet Synchronous Machine, Efficiency.**

I. INTRODUCTION

As modern electronic technology improves, the aviation sector is increasingly attentive to the concept of "*More Electric Aircraft*" [1]. An electric power system can usually provide much better flexibility and diagnosis is easier than with mechanical systems such as those using hydraulic and pneumatic power. This will lead to reductions in weight and maintenance costs.

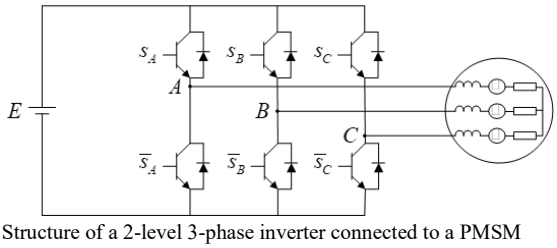

Fig. 1 Structure of a 2-level 3-phase inverter connected to a PMSM

In a control system, the actuator is the key element that converts energy (electric, hydraulic, pneumatic, etc.) to mechanical motion. The PMSM is the most widely-used system because it has proved to be particularly efficient in areas such as high power density and because it has a good dynamic performance [2]. An actuator system is constructed by coupling a PMSM with an inverter (Fig. 1). Through modulating the switching state of the inverter, the desired position, speed and torque can be obtained.

Multiple actuators are often assigned to drive the same object, such as an elevator, a spoiler or a flap in aeronautical applications. This evenly distributes the drive force on a long, thin control surface thereby increasing the effective aerodynamic force and reducing structural weight. In these situations, the speed and position of each actuator must be synchronous. Due to the "auto-pilot" characteristic of PMSM, its speed and position are always synchronous with the electrical frequency applied. Connecting PMSMs in parallel creates a dependency in speed and position between the two machines but reduces the weight and complexity of the control electronics. This type of configuration is illustrated in Fig. 2 with two PMSMs.

Although these machines have the same speed and position, they must be subjected to different load torques. As a fundamental feasibility test [3] has demonstrated, the ability to control independent torques comes from the electrical angle displacement between two machines. Some research [4]-[8] has used "*equivalent machine*" techniques which transform the two machines into a single machine by taking the average speed, position and current values. Among them [7] have proposed a more advanced "*mean and difference*" technique optimizing the transient performance. On the other hand, the "*master slave*" technique [8] only controls the machine with a higher load torque at each instant while the other one is left open loop. Model Predictive Control (MPC) is now very

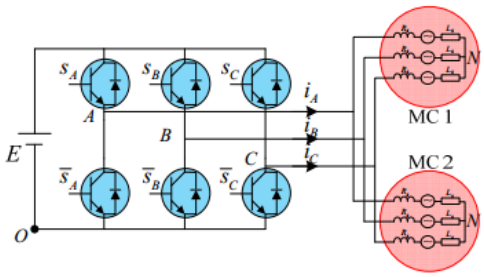

Fig. 2 A 2-level 3-phase inverter driving 2 PSMSs in parallel

popular and it is also envisaged for MIDPMSM. [9]-[12] propose Optimal Predictive Torque Control (OPTC) which handles this system directly using optimal voltage vector prediction. It transforms the control problem into an optimization problem by minimizing a cost function which takes both torque reference and system efficiency into account

This article has been accepted for publication in a future issue of this journal, but has not been fully edited. Content may change prior to final publication. Citation information: DOI 10.1109/TIA.2017.2768535, IEEE Transactions on Industry Applications

at the same time.

Meanwhile, the efficiency problem is important for real applications. Articles [13] and [14] have shown that the efficiency of the MIDPMSM system without optimization can be very low (about 40%) while for a single-machine system the efficiency is usually very high (> 90%) by applying an MTPA (Maximum Torque Per Ampere) strategy. Optimization for 2 machines is more complex because it is impossible to set the stator flux perpendicular to both machines' rotor flux at the same time. [15] gives an analytical analysis in optimal efficiency by maximizing the ratio between total torque and total current. But its actual optimal point can be calculated only by using the numerical method. In [16] the optimal operating point is analytically calculated by the steady state model. I_{d1} is used to bring the system to the calculated point. [17] has designed a controller by positing the existence of steady state solution. One redundant degree of freedom can be used to bring the system to the optimal efficiency state. But it lacks stability of analysis and its optimal point is obtained using the exhaustive method.

The purpose of this paper is to propose a comprehensive yet simple efficiency-optimal controller solution to the MIDPMSM system. System controllability, determinacy and stability limitations of this controller are studied and proved. Moreover, an analytical calculation of the optimal point is given. During the experimental part, its feasibility and stability are verified; its efficiency is better than existing control strategies.

II. Steady State Model of an MIDPMSM System

The model of an MIDPMSM system must be defined before proceeding to its analysis. In this paper a non-salient pole PMSM is considered. This assumption means the sinusoidal electromotive force, negligible magnetic losses and cogging torque and the magnetic circuit operates in the linear region. To simplify the analysis, two machines are presumed to be identical and operate at the same speed in steady-state. However, this may not be the case as the speed of each machine may vary during a transient. Both machines are powered by the same voltage system so the steady-state speeds are the same. In transient mode, the speeds may be different, especially if the load torques are different. Defining the d axis of a d-q frame aligns with the flux of the rotor, the steady state model of machine 1 can be expressed as follows:

$$\begin{bmatrix} V_{d1} \\ V_{q1} \end{bmatrix} = \begin{bmatrix} R_s & -L_s\omega_e \\ L_s\omega_e & R_s \end{bmatrix} \begin{bmatrix} I_{d1} \\ I_{q1} \end{bmatrix} + \begin{bmatrix} 0 \\ \omega_e\varphi_p \end{bmatrix} \quad (1)$$

where:

V_d, V_q: Stator Voltage.

I_d, I_q: Stator Current.

L_s: Stator windings inductance.

φ_p: Permanent magnets flux.

R_s: Stator resistance.

ω_e: Electrical speed.

For machine 2, $\vec{V}_{dq}$ must be mapped into its coordinate since there is electrical angle displacement between the two machines. To define $\theta_d = \theta_2 - \theta_1$, where θ_1 and θ_2 correspond to the electrical angle of each machine, the steady state model for machine 2 can be expressed as:

$$\begin{bmatrix} cos\,\theta_d & sin\,\theta_d \\ -sin\,\theta_d & cos\,\theta_d \end{bmatrix} \begin{bmatrix} V_{d1} \\ V_{q1} \end{bmatrix} = \begin{bmatrix} R_s & -L_s\omega_e \\ L_s\omega_e & R_s \end{bmatrix} \begin{bmatrix} I_{d2} \\ I_{q2} \end{bmatrix} + \begin{bmatrix} 0 \\ \omega_e\varphi_p \end{bmatrix} \quad (2)$$

Then the model of the MIDPMSM system can be obtained through merging (1) and (2). The steady-state model of the MIDPMSM system is shown in (3).

$$\begin{bmatrix} 1 & 0 \\ 0 & 1 \\ cos\,\theta_d & sin\,\theta_d \\ -sin\,\theta_d & cos\,\theta_d \end{bmatrix} \begin{bmatrix} V_{d1} \\ V_{q1} \end{bmatrix} = \begin{bmatrix} R_s & -\omega_e L_s & 0 & 0 \\ \omega_e L_s & R_s & 0 & 0 \\ 0 & 0 & R_s & -\omega_e L_s \\ 0 & 0 & \omega_e L_s & R_s \end{bmatrix} \begin{bmatrix} I_{d1} \\ I_{q1} \\ I_{d2} \\ I_{q2} \end{bmatrix} + \begin{bmatrix} 0 \\ \omega_e\varphi_p \\ 0 \\ \omega_e\varphi_p \end{bmatrix} \quad (3)$$

III. Proposed Control Strategy

A. System determinacy and controller architecture

An undetermined system is difficult to analyse because its behaviour is unpredictable. It must first be considered in the controller design phase because it affects the structure of the controller. The steady-state model (3) shows that the MIDPMSM system has two input variables (V_{d1}, V_{q1}) and six state variables (I_{q1}, I_{q2}, I_{d1}, I_{d2}, θ_d, ω_e). Amongst them the torque and speed (I_{q1}, I_{q2}, ω_e) are defined by external requirements. They must be treated as known variables in (3). Thus in (3) there are 5 unknown variables left but only 4 equations available. As described in [17], the input voltage remains undetermined (solution number is infinity) unless the controller chose an additional variable under control amongst I_{d1}, I_{d2} or θ_d so that the input voltage is determined (solution number is finite).

This additional controlled variable can be used to bring the system to its efficiency-optimal state if it is set to the same value as when it is in the optimal state. Here θ_d is selected as the controlled variable. The steady-state mode (3) can be rewritten in the non-homogeneous linear equation form (shown in (4)).

$$\begin{bmatrix} -R_s & 0 & 1 & 0 \\ -\omega_e L_s & 0 & 0 & 1 \\ 0 & -R_s & cos\,\theta_d & sin\,\theta_d \\ 0 & -\omega_e L_s & -sin\,\theta_d & cos\,\theta_d \end{bmatrix} \begin{bmatrix} I_{d1} \\ I_{d2} \\ V_{d1} \\ V_{q1} \end{bmatrix} = \begin{bmatrix} -\omega_e L_s I_{q1} \\ R_s I_{q1} + \omega_e\varphi_p \\ -\omega_e L_s I_{q2} \\ R_s I_{q2} + \omega_e\varphi_p \end{bmatrix} \quad (4)$$

Its corresponding solution is:

$$\begin{cases} I_{d1} = \dfrac{Ay - B}{Z^2 x} - \dfrac{C}{Z^2} \\ I_{d2} = \dfrac{A - By}{Z^2 x} - \dfrac{C}{Z^2} \\ V_{d1} = y\left(R_s I_{d2} - \omega_e L_s I_{q2}\right) - x\left(R_s I_{q2} + \omega_e L_s I_{d2} + \omega_e\varphi_p\right) \\ V_{q1} = x\left(R_s I_{d2} - \omega_e L_s I_{q2}\right) + y\left(R_s I_{q2} + \omega_e L_s I_{d2} + \omega_e\varphi_p\right) \end{cases} \quad (5)$$

where

This article has been accepted for publication in a future issue of this journal, but has not been fully edited. Content may change prior to final publication. Citation information: DOI 10.1109/TIA.2017.2768535, IEEE Transactions on Industry Applications

$$\begin{cases} Z = \sqrt{{R_s}^2 + (\omega_e L_s)^2} \\ A = Z^2 I_{q1} + R_s \omega_e \varphi_p \\ B = Z^2 I_{q2} + R_s \omega_e \varphi_p \\ C = L_s {\omega_e}^2 \varphi_p \\ x = sin\,\theta_d \\ y = cos\,\theta_d \end{cases} \quad (6)$$

Fig. 3 shows the proposed controller block diagram. The controller consists of two blocks: master motor controller and θ_d regulator. The master controller only controls machine 1. Machine 2 is left open loop. In the master controller, a regular vector current controller is used. Space Vector Modulation [18] (SVM) generates the desired voltage vector. The I_{q1} reference is given by a PI speed controller. The I_{d1} reference is given by the θ_d regulator. The principle of the controller is to:

1) Calculate the optimal steady-state through θ_d.
2) Obtain the system state by (5).
3) Set I_{d1}^* to the same value as that in the optimal state.

Steps 2 and 3 are processed by the θ_d regulator. This method uses θ_d to calculate the optimal system state because taking θ_d as a known variable makes the state solution of (3) linear and unique. This property simplifies the analysis and results greatly. Moreover, the state is set by I_{d1} which is easier to implement.

B. Stability

However, it must be proved beforehand that the I_{d1} set can drive the system only to the given state (that the response is unique).

This precondition is linked to the solution condition of an

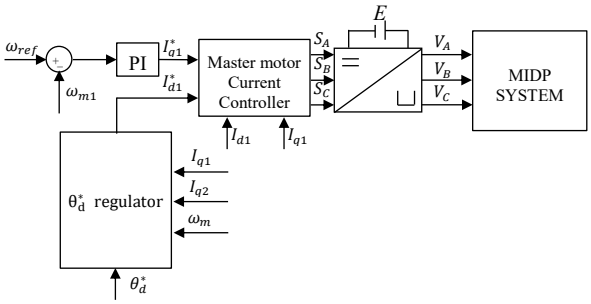

Fig. 3 Block diagram of proposed controller

MIDPMSM system for a given I_{d1} and its stability. Here a graph-based demonstration is given to illustrate this. The corresponding mathematical proof can be found in the Appendix.

Firstly, the solution condition is analyzed. Fig. 4(a) shows the I_d current response with respect to θ_d when machine 1 is more loaded, A>B in (6). It is easy to identify that for a given I_{d1}, there are always two possible θ_d located in the negative plane and the positive plane respectively. Fig. 4(b) shows the curve of I_{d1} when machine 2 is more loaded; it has a hyperbola shape. Obviously, either I_{d1} is in the upper or lower plane, there are at most two possible θ_d. The extreme values (shown as red point in Fig. 4(b)) are:

$$\theta_d^{critical} = \pm \cos^{-1}\left(\frac{A}{B}\right) \quad A < B \quad (7)$$

In the second step, the stability of machine 2 must be studied because it operates in open-loop mode. It can only converge to a stable steady state. The proof of stability is based on the conclusion of [8]. Defining the angle between voltage vector

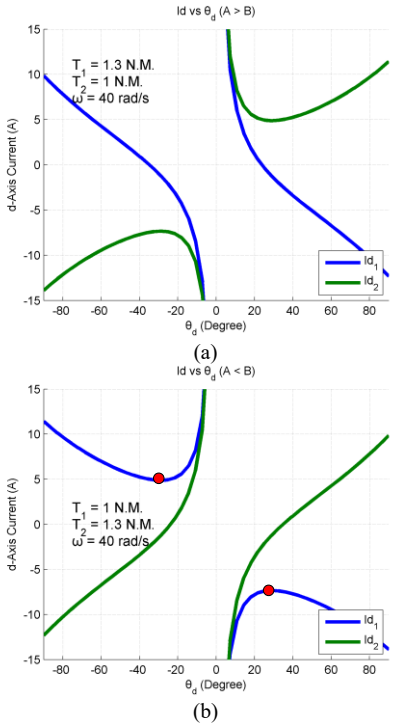

Fig. 4 Typical curve of Id response respect to θ_d.

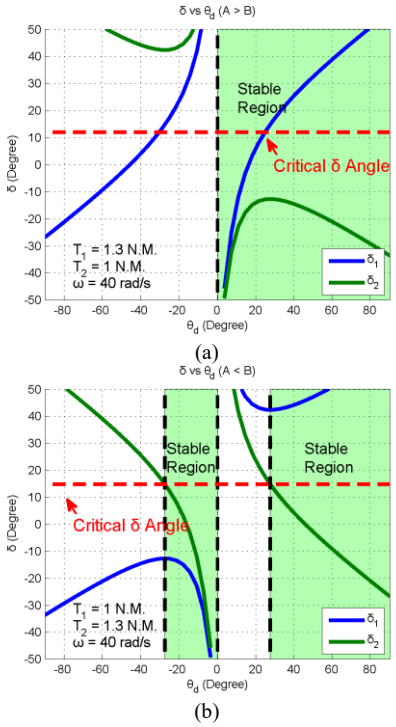

Fig. 5 Typical curve of δ response respect to θ_d.

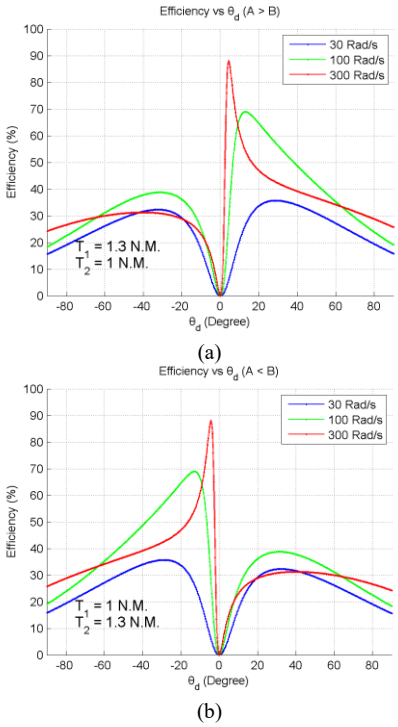

Fig. 6 Typical curve of system efficiency respect to θ_d under different speed and torque.

This article has been accepted for publication in a future issue of this journal, but has not been fully edited. Content may change prior to final publication. Citation information: DOI 10.1109/TIA.2017.2768535, IEEE Transactions on Industry Applications

and the back-EMF vector as δ, for a general PMSM its stable region is:

$$-\pi + \alpha < \delta < \alpha \tag{8}$$

where $\alpha = \tan^{-1}\frac{\omega_e L_s}{R_s}$ in a forward rotating situation. Fig. 5(a) shows δ angle of each machine with respect to θ_d when machine 1 is more loaded (A>B). The red dotted line represents the critical α angle. If focus is on machine 2, its stability is achieved when δ_2 is below the red dotted line. It is represented as the green area in the various figures. Fig. 5(b) shows the curve when machine 2 is more loaded (A<B). The stable region is $\left(-\cos^{-1}\left(\frac{A}{B}\right), 0\right) \cup \left(\cos^{-1}\left(\frac{A}{B}\right), \frac{\pi}{2}\right)$. The intersecting points between δ_2 and α coincide with the extreme points of I_{d1} in Fig. 4(b). It shall be noticed that in the right part of this stable region, which is $\left(\cos^{-1}\left(\frac{A}{B}\right), \frac{\pi}{2}\right)$, motor 1 is open-loop instable. Controller for motor 1 must be capable of manipulating the master motor under instable condition. Otherwise, this part must not be considered as a valid stable region.

The analysis of the solution condition illustrates that for a given I_{d1}, there are at most two corresponding steady states. And only one of these corresponds to the given state. But if stability is taken into account, only one steady state remains. The conclusion is represented in Fig. 7. θ_d^1 and θ_d^2 represent the two possible solutions for a given I_{d1} respectively. It is easy to identify that, in each case, only one stable solution is available. It can therefore be concluded that the precondition only holds true when θ_d^* is in the stable region, which is:

$$\theta_d^* \in \begin{cases} \left(-\cos^{-1}\left(\frac{A}{B}\right), 0\right) \cup \left(\cos^{-1}\left(\frac{A}{B}\right), \frac{\pi}{2}\right) & A < B \\ \left(0, \frac{\pi}{2}\right) & A \geq B \end{cases} \tag{9}$$

C. *Efficiency Optimization*

The efficiency is optimized by minimizing the loss of Joules from the motor. It can be expressed as:

$$P_{joule\ loss} = R_s\left({I_{q1}}^2 + {I_{q2}}^2 + {I_{d1}}^2 + {I_{d2}}^2\right) \tag{10}$$

Because the torques are determined externally, Joule loss due to I_q cannot be reduced; Joule loss due to I_d must be reduced to increase the efficiency. Defining a cost function as

$$supplementary\ joule\ loss = R_s \cdot \left({I_{d1}}^2 + {I_{d2}}^2\right) \tag{11}$$

Refer back to (5), θ_d is the only degree of freedom that minimizes this cost function. The analytical solution of the optimal θ_d can be obtained using the Lagrange multiplier method.

Insert (5) into (11), the cost function can be rewritten as

$$f(x,y) = \left(\frac{Ay - B}{Z^2 x} - \frac{C}{Z^2}\right)^2 + \left(\frac{A - By}{Z^2 x} - \frac{C}{Z^2}\right)^2 \tag{12}$$

As $\sin\theta_d = x$ and $\cos\theta_d = y$, this cost function must be subjected to constraint (13).

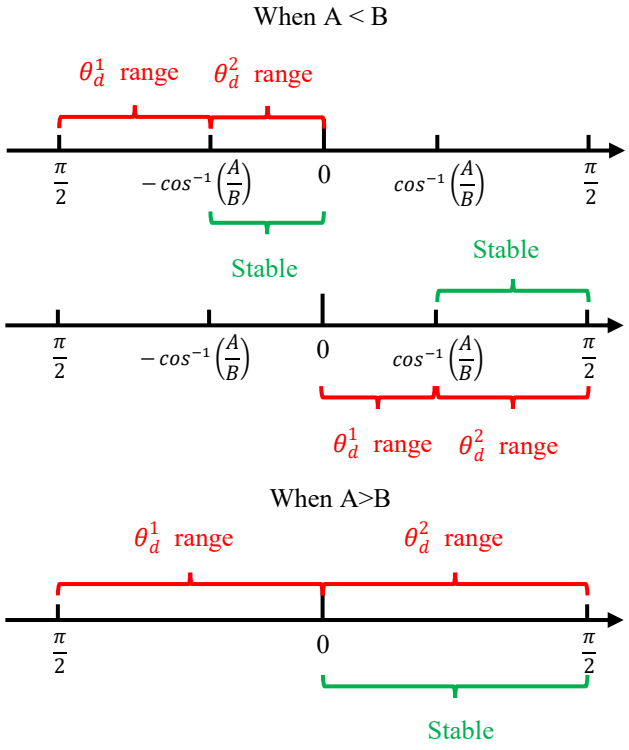

Fig. 7 Illustration of proof

$$g(x,y) = x^2 + y^2 = 1 \tag{13}$$

Then Lagrange multipliers can be used to identify the extreme point of (12), which are the candidates for being the optimal θ_d.

$$L(x,y,\lambda) = f(x,y) + \lambda(g(x,y) - 1) \tag{14}$$

Making partial derivation of (14), which is shown below,

$$\begin{aligned} \frac{\partial L(x,y,\lambda)}{\partial x} &= 8ABy - 2(y+1)(BC - AC)x + 2\lambda Z^4 x^4 - 4(A^2 + B^2) = 0 \\ \frac{\partial L(x,y,\lambda)}{\partial y} &= 4AB - 2(BC - AC)x - 2\lambda Z^2 y x^2 = 0 \\ \frac{\partial L(x,y,\lambda)}{\partial \lambda} &= x^2 + y^2 - 1 = 0 \end{aligned} \tag{15}$$

the optimal θ_d is one of the solutions of (15). Finally, a quartic function (16) can be obtained.

$$x^4 + \alpha x^3 + \beta x^2 + \gamma x - \beta = 0 \tag{16}$$

where

$$\begin{cases} \alpha = \dfrac{4C(B^3 - A^3)}{4A^2B^2 + (BC - AC)^2} \\ \beta = \dfrac{4(B^2 - A^2)^2}{4A^2B^2 + (BC - AC)^2} \\ \gamma = \dfrac{4C\left((A - B)(A + B)^2\right)}{4A^2B^2 + (BC - AC)^2} \end{cases} \tag{17}$$

this equation can be solved using the Ferrari method, similar to [19]. Fig. 6 shows a typical curve of system efficiency with respect to θ_d. It illustrates the efficiency of the system at different speeds whilst the torque speed remains constant. Judging from Fig. 6, there are two extreme points in the left and right panel respectively. It can be concluded that, amongst

This article has been accepted for publication in a future issue of this journal, but has not been fully edited. Content may change prior to final publication. Citation information: DOI 10.1109/TIA.2017.2768535, IEEE Transactions on Industry Applications

these four solutions, there are two real solutions and two complex solutions. The real solutions are related to the two extreme points. The optimization procedure is defined as:

1) Calculate A, B, C using (6).
2) Calculate α, β, γ using (17).
3) Calculate the solutions of (16).
4) Ignore the two complex solutions. For the two real solutions, use (5) to calculate the corresponding I_d current and compare their cost function value.
5) Set the optimal $\theta_d = \sin^{-1} x$.

IV. Experiment and Comparison

An experiment was carried out to verify the feasibility and to illustrate the performance of the proposed controller. The experimental bench is illustrated in Fig. 8. Three PMSMs were used. PMSM 1 and PMSM 2 are the experimental motors, they are identical. Each of them is equipped with a position encoder to measure rotor position and current sensors. The motor located between them is used as a controllable load torque generator. It is connected to a commercial PMSM controller and its torque can be configured by imposing a current. Each of the three PMSMs is connected to a linear ball screw actuator and drives its own axis. In this experiment, the axis of PMSM 1 was rigidly connected to the axis of the generator. As the optimization processes and stability determination relays on correct observation of torque and speed, when any one of the motors is stopped, its torque cannot be estimated (output torque always smaller than static friction). To start the motors correctly, the Master-Slave strategy is used because it uses θ_d to determine their torque relationship directly. Once their mechanical speed is higher than 5rad/s, the optimization processes are executed. The parameters of the machine are given in TABLE I.

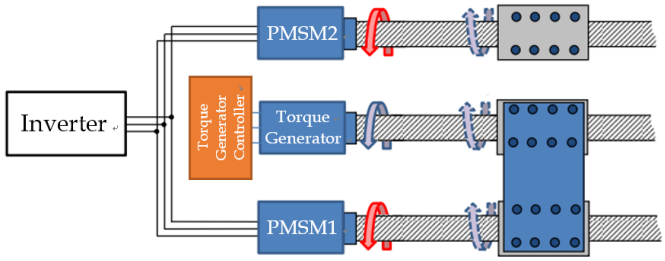

Fig. 8 The configuration of the experimental bench

A. Stability demonstration

Fig. 9 demonstrates the precondition obtained in section III. A ramp-shaped reference θ_d^* changing from $-\frac{\pi}{6}$ to $\frac{\pi}{6}$ is put into the θ_d regulator. Judging from the current response, machine 1 is more loaded (A>B) therefore the stable region is $\left(0, \frac{\pi}{2}\right)$. In Fig. 9(a), when θ_d^* is in the stable region, the θ_d response follows. When θ_d^* is in an unstable region, the response remains in the stable region. Fig. 9(b) demonstrates this principle. If a reference in an unstable region is given (indicated as θ_d^*), the θ_d regulator will generate a corresponding I_{d1}^*. But the slave machine will converge to the θ_d in the stable region having the same I_{d1}^*.

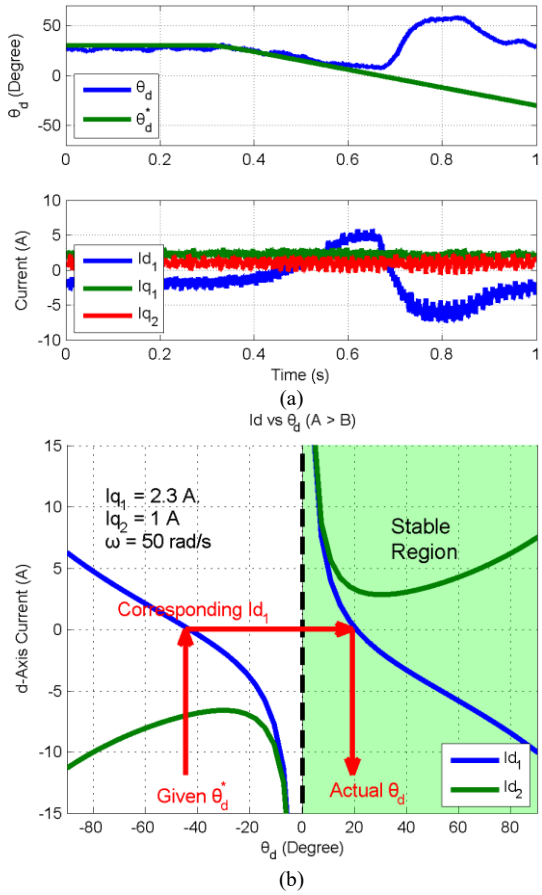

Fig. 9 Demonstration of stability conclusion

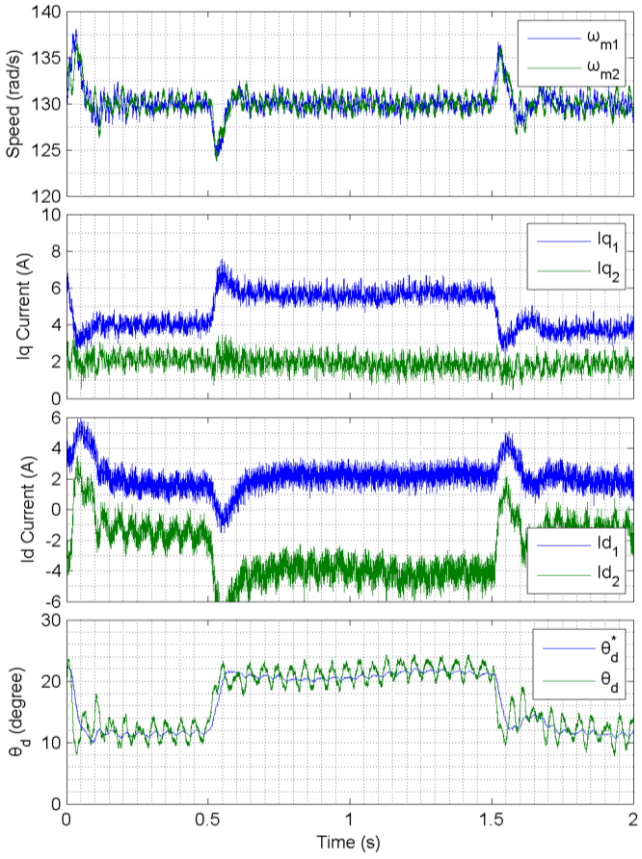

Fig. 10 Results of efficiency test

This article has been accepted for publication in a future issue of this journal, but has not been fully edited. Content may change prior to final publication. Citation information: DOI 10.1109/TIA.2017.2768535, IEEE Transactions on Industry Applications

B. *Efficiency test*

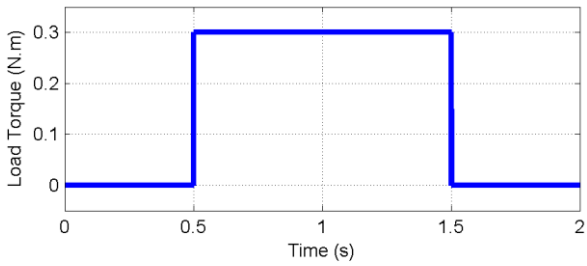

Fig. 11 Load torque applied to machine 1

Fig. 10 shows the experiment results of the efficiency test. During the experiment, the two machines were first put in steady speed operation. Then, an external load torque was applied to machine 1 in order to test the system transient, its robustness, and its efficiency in the case of different load torque. Its shape is shown in Fig. 11. The load torque was not applied to machine 2.

Fig. 10 shows the corresponding θ_d response (green curve). The blue curve is the optimal θ_d realtime calculated during execution. It follows the reference well confirming the effetiveness of the θ_d regulator. The oscillations of θ_d are linked to the mechanical imperfections of the system and in particular to a periodic variation of the friction.

Moreover, as the objective is to optimize efficiency, it is interesting to compare the new proposed control strategy with other strategies. The efficiency is calculated as

$$\eta = \frac{\omega_e \varphi_p (I_{q1} + I_{q2})}{\omega_e \varphi_p (I_{q1} + I_{q2}) + R_s (I_{d1}^2 + I_{q1}^2 + I_{d2}^2 + I_{q2}^2)} \quad (18)$$

As tested in [13];[14], master slave is the best efficiency strategy. Now we take this reference to test our new proposal. The result is shown in Fig. 12. The blue curve represents the estimated maximum efficiency obtained by the optimization procedure; it is calculated by the estimated I_{d1} and I_{d2} through (5).

$$\eta_{theory} = \frac{\omega_e \varphi_p (I_{q1} + I_{q2})}{\omega_e \varphi_p (I_{q1} + I_{q2}) + R_s (\hat{I}_{d1}^2 + \hat{I}_{d2}^2 + I_{q1}^2 + I_{q2}^2)} \quad (19)$$

The red curve shows the efficiency of the new strategy. The black curve is that of the master slave. It can be concluded that the new control strategy provides even higher efficiency. Meanwhile the efficiency of the new strategy is almost the same as the estimated theoretical efficiency. This proves the correctness of optimization process.

V. CONCLUSION

In this paper an efficiency optimized controller for an MIDPMSM system is proposed. The analysis of the existence of a steady state solution has given out the design guideline to the controller structure. The use of the intermediary variables θ_d greatly simplifies the optimization process and the stability criterion. Moreover, the analytical solution of the maximum efficiency operation point is given so that the costly computational numerical method can be avoided. The experiment has proved these criteria and the effectiveness of the optimization.

TABLE I
PARAMETERS OF PMSM

Symbol	Description	Value
V_{dc}	Voltage of the DC bus	30V
I_n	Nominal Current	4.3A
P_n	Nominal Power	913W
f_{dec}	Current Control frequency	10 kHz
R_s	Stator resistance	1.25 Ω
L_s	Cyclic inductance	1.65 mH
φ_p	Amplitude of the flux due to the magnets	0.039 Wb
N_p	Number of pairs of poles	4
K_c	Torque constant	0.32 Nm/A

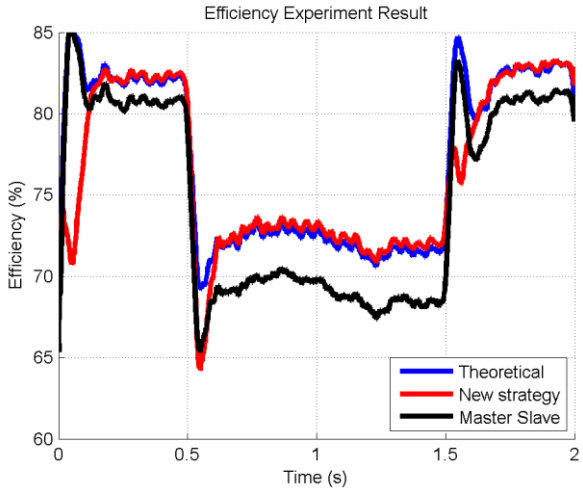

Fig. 12 Comparison of performance between different controllers

Above all, the controller structure is simple. Regular controllers for a single PMSM system can be easily upgraded to support parallel PMSM just by adding a few blocks without modifying the controller itself. But there is still room for improvement. Open-loop efficiency optimization is used here which relies heavily on the accuracy of system parameters. These parameters may change when the system is in operation. It would be interesting to implement a closed loop optimization to make it robust.

APPENDIX

The proof assumes that:

- The rotational speed is positive.
- Both machines operate as motor, which means A and B in (6) are positive.

A. *Situation of θ_d with respect to I_{d1}*

In the first step, the situation of θ_d with respect to I_{d1} will be studied. Recalling the expression of θ_d with respect to I_{d1}.

$$I_{d1} = \frac{A \cos\theta_d - B}{Z^2 \sin\theta_d} - \frac{C}{Z^2} \quad (20)$$

Defining the value range of θ_d as $\left(-\frac{\pi}{2}, \frac{\pi}{2}\right)$, $\cos\theta_d$ and $\sin\theta_d$ in (20)) can be replace by

This article has been accepted for publication in a future issue of this journal, but has not been fully edited. Content may change prior to final publication. Citation information: DOI 10.1109/TIA.2017.2768535, IEEE Transactions on Industry Applications

$$\begin{cases} cos\,\theta_d = \sqrt{1-k^2} \\ sin\,\theta_d = k \end{cases} \quad (21)$$

Then (20) can be transferred into a quadratic equation respect to k. After arrangement, the equation becomes:

$$((I_{d1}Z^2 + C)^2 + A^2)k^2 + 2(I_{d1}Z^2B + BC)k + B^2 - A^2 = 0 \quad (22)$$

The corresponding solution of k is shown below.

$$\begin{cases} k_1 = \dfrac{-(I_{d1}Z^2 + C)B + A\sqrt{A^2 - B^2 + (I_{d1}Z^2 + C)^2}}{(I_{d1}Z^2 + C)^2 + A^2} \\ k_2 = \dfrac{-(I_{d1}Z^2 + C)B - A\sqrt{A^2 - B^2 + (I_{d1}Z^2 + C)^2}}{(I_{d1}Z^2 + C)^2 + A^2} \end{cases} \quad (23)$$

If (23) are real solutions, this means the discriminant under the square root should be greater or equal to zero. It can be expressed by the inequality in (24).

$$Z^4 {I_{d1}}^2 + 2CZ^2 I_{d1} + C^2 + A^2 - B^2 \geq 0 \quad (24)$$

(24) can be seen as a quadratic function with respect to I_{d1}. Since Z^2 is always positive, this quadratic function has an open up-shaped curve. Obviously, when there is no intersection between the curve and the x axis (or I_{d1} axis in this case), (23) is always satisfied. When there are two intersections, the solution is

$$(-\infty, r1] \cup [r2, +\infty) \quad (25)$$

Thus it is necessary to discuss the discriminating relationship which is:

$$\Delta = 4Z^2(B^2 - A^2) \quad (26)$$

1) $\Delta < 0$

This is equivalent to A>B, which means machine 1 is more loaded. In this situation (24) is always satisfied. This represents the situation in Fig.5(a).

2) $\Delta \geq 0$

In this case the solution of (22) is

$$I_{d1} \in \left(-\infty, \frac{-C - \sqrt{B^2 - A^2}}{Z^2}\right) \cup \left(\frac{-C + \sqrt{B^2 - A^2}}{Z^2}, +\infty\right) \quad (27)$$

This represents the situation in fig.5 (b). It is easy to calculate the critical θ_d.

$$\theta_d^{critical} = \pm \cos^{-1}\left(\frac{A}{B}\right) \quad (28)$$

To summarise, for each given I_{d1} reference, depending on the torque relationship of the two machines, there are two possible θ_d located in $\left(-\frac{\pi}{2}, 0\right)$ and $\left(0, \frac{\pi}{2}\right)$ respectively. If I_{d1} reference is in $\left(-\infty, \frac{-2C-\sqrt{B^2-A^2}}{Z^2}\right)$, there are two possible θ_d in $\left(-\frac{\pi}{2}, -\cos^{-1}\left(\frac{A}{B}\right)\right)$ and $\left(-\cos^{-1}\left(\frac{A}{B}\right), 0\right)$ respectively. Otherwise if I_{d1} is in $\left(\frac{-2C+\sqrt{B^2-A^2}}{Z^2}, +\infty\right)$, the two possibilities would be in $\left(0, \cos^{-1}\left(\frac{A}{B}\right)\right)$ and $\left(\cos^{-1}\left(\frac{A}{B}\right), \frac{\pi}{2}\right)$.

In conclusion, for a given I_{d1}, there are at most two corresponding θ_d. When $A > B$, there are always two solutions. When $A < B$, there are two solutions when I_{d1} satisfies (27).

B. Stable region

When δ is defined in $\left(-\frac{\pi}{2}, \frac{\pi}{2}\right)$, it is interesting to compare the tangent values of δ_2 and α directly.

$$tan\,\delta_2 = -\frac{V_{d2}}{V_{q2}} < \frac{L_s\omega_e}{R_s} \quad (29)$$

Refer to (1), we can replace V_{d2} and V_{q2} with the expression respect to the current, which is:

$$-\frac{V_{d2}}{V_{q2}} = -\frac{R_sI_{d2} - L_s\omega_eI_{q2}}{L_s\omega_eI_{d2} + R_sI_{q2} + \omega_e\varphi_p} < \frac{\omega_eL_s}{R_s} \quad (30)$$

Both sides of (30) must multiply $V_{q2}R_s$ to cancel the fraction. R_s is a positive number. Thus, the value of V_{q2} must be specified. Regarding the assumption, V_{q2} is always greater than zero, which is equivalent to (31).

$$I_{d2} > -\frac{R_sI_{q2} + \omega_e\varphi_p}{L_s\omega_e} \quad (31)$$

Taken the precondition (31) into consideration, the solution of (30) is:

$$I_{d2} > -\frac{C}{Z^2} \quad (32)$$

The final result is determined by the Intersection of (31) and (32). They have the same sign so it is necessary to compare the constant term in the right side of them, which is $-\frac{R_sI_{q2}+\omega_e\varphi_p}{L_s\omega_e}$ and $-\frac{C}{Z^2}$, to determine the final result. Making subtract between them, the result is:

$$-\frac{R_sI_{q2} + \omega_e\varphi_p}{L_s\omega_e} - \left(-\frac{C}{Z^2}\right) = -\frac{\left({R_s}^3 + (\omega_eL_s)^2R_s\right)I_{q2} + {R_s}^2\omega_e\varphi_p}{L_s\omega_e\left({R_s}^2 + (\omega_eL_s)^2\right)} \quad (33)$$

Obviously (33) is smaller than zero if the assumptions are taken into account. This means that the constant term in the right side of (31) is smaller than (32). Thus, the stable region should be (32).By replacing I_{d2} in (32) with the equation in (6), the stable region respect to θ_d is determined by (34).

$$\frac{A - B\,cos\,\theta_d}{Z^2\,sin\,\theta_d} > 0 \quad (34)$$

Discussion on $\sin\theta_d$ should be made. When $\sin\theta_d > 0$, which corresponds to $\theta_d \in \left(0, \frac{\pi}{2}\right)$, $Z^2\sin\theta_d$ can be multiplied without changing the sign of (34). (34) becomes:

$$cos\,\theta_d < \frac{A}{B} \quad (35)$$

In this situation, relationship between A and B must discussed. The result is shown in (36).

$$\begin{cases} \left(cos^{-1}\left(\frac{A}{B}\right), \frac{\pi}{2}\right) & A < B \\ \left(0, \frac{\pi}{2}\right) & A \geq B \end{cases} \tag{36}$$

On the other hand, when $\sin\theta_d < 0$, which corresponds to $\theta_d \in \left(-\frac{\pi}{2}, 0\right)$, (34) becomes:

$$cos\,\theta_d > \frac{A}{B} \tag{37}$$

Its solution is:

$$\begin{cases} \left(-cos^{-1}\left(\frac{A}{B}\right), 0\right) & A < B \\ \emptyset & A \geq B \end{cases} \tag{38}$$

Merging (36) and (38), the stable region of θ_d can be obtained.

$$\begin{cases} \left(-cos^{-1}\left(\frac{A}{B}\right), 0\right) \cup \left(cos^{-1}\left(\frac{A}{B}\right), \frac{\pi}{2}\right) & A < B \\ \left(0, \frac{\pi}{2}\right) & A \geq B \end{cases} \tag{39}$$

REFERENCES

[1] B. Sarlioglu and C. Morris, "More Electric Aircraft – Review, Challenges and Opportunities for Commercial Transport Aircraft", Transportation Electrification, IEEE Transactions on , vol.PP, no.99, pp.1, May, 2015.

[2] T. Inoue, Y. Inoue, S. Morimoto and M. Sanada, "Mathematical Model for MTPA Control of Permanent-Magnet Synchronous Motor in Stator Flux Linkage Synchronous Frame," in *IEEE Transactions on Industry Applications*, vol. 51, no. 5, pp. 3620-3628, Sept.-Oct. 2015.

[3] J.Chiasson, Danbing Seto, Fanping Sun, A. Stankovic and S. Bortoff, "Independent control of two PM motors using a single inverter: application to elevator doors," *Proceedings of the 2002 American Control Conference (IEEE Cat. No.CH37301)*, Anchorage, AK, USA, 2002, pp. 3093-3098 vol.4.

[4] A.Asri, D. Ishak, S. Iqbal and M. Kamarol, "A speed sensorless field oriented control of parallel- connected dual PMSM," *Control System, Computing and Engineering (ICCSCE), 2011 IEEE International Conference on*, Penang, 2011, pp. 567-570.

[5] AhmadAsri Abd Samat, D. Ishak, P. Saedin and S. Iqbal, "Speed-sensorless control of parallel- connected PMSM fed by a single inverter using MRAS," *Power Engineering and Optimization Conference (PEDCO) Melaka, Malaysia, 2012 Ieee International*, Melaka, 2012, pp. 35-39.

[6] J.M. Lazi, Z. Ibrahim, M. H. N. Talib and R. Mustafa, "Dual motor drives for PMSM using average phase current technique," *Power and Energy (PECon), 2010 IEEE International Conference on*, Kuala Lumpur, 2010, pp. 786-790.

[7] M.S. D. Acampa, A. Del Pizzo and D. Iannuzzi, "Optimized control technique of single inverter dual motor AC-brushless drives," *2008 43rd International Universities Power Engineering Conference*, Padova, 2008, pp. 1-6.

[8] D.Bidart, M. Pietrzak-David, P. Maussion and M. Fadel, "Mono inverter multi-parallel permanent magnet synchronous motor: structure and control strategy," in *IET Electric Power Applications*, vol. 5, no. 3, pp. 288-294, March 2011.

[9] N.L. Nguyen, M. Fadel and A. Llor, "A new approach to Predictive Torque Control with Dual Parallel PMSM system," *Industrial Technology (ICIT), 2013 IEEE International Conference on*, Cape Town, 2013, pp. 1806-1811.

[10] M.Fadel, N. L. Nguyen and A. Llor, "Different solutions of predictive control for two synchronous machines in parallel," *2013 IEEE International Symposium on Sensorless Control for Electrical Drives and Predictive Control of Electrical Drives and Power Electronics (SLED/PRECEDE)*,

[11] N.L. Nguyen, M. Fadel and A. Llor, "Predictive Torque Control - A solution for mono inverter-dual parallel PMSM system," *2011 IEEE International Symposium on Industrial Electronics*, Gdansk, 2011, pp. 697-702.

[12] A. Bouarfa, M. Fadel, "Optimal Predictive Torque Control of Two PMSM supplied in Parallel on a Single Inverter", in Control of Power and Energy Systems (CPES), 2015, Volume 48, Issue 30, p.p.84-89.

[13] T.Liu and M. Fadel, "Performance comparison of control strategies for mono-inverter Dual-PMSM system," *2016 IEEE International Power Electronics and Motion Control Conference (PEMC)*, Varna, 2016, pp. 637-642.

[14] T.Liu and M. Fadel, "Comparative study of different predictive torque control strategies for mono-inverter dual-PMSM system," *2016 18th Mediterranean Electrotechnical Conference (MELECON)*, Lemesos, 2016, pp. 1-6.

[15] A.Del Pizzo, D. Iannuzzi and I. Spina, "High performance control technique for unbalanced operations of single-vsi dual-PM brushles motor drives," *2010 IEEE International Symposium on Industrial Electronics*, Bari, 2010, pp. 1302-1307.

[16] Y.Lee and J. I. Ha, "Control Method for Mono Inverter Dual Parallel Surface-Mounted Permanent-Magnet Synchronous Machine Drive System," in *IEEE Transactions on Industrial Electronics*, vol. 62, no. 10, pp. 6096-6107, Oct. 2015.

[17] T.Liu and M. Fadel, "An Efficiency Optimizing Controller Design Method for Mono-Inverter Dual-PMSM System," 2016 *IEEE International Conference on Power Electronics, Drives and Energy System*, Trivandrum, 2016, in press.

[18] F. Zhang, L. Zhu, S. Jin, W. Cao, D. Wang and J. L. Kirtley, "Developing a New SVPWM Control Strategy for Open-Winding Brushless Doubly Fed Reluctance Generators," in *IEEE Transactions on Industry Applications*, vol. 51, no. 6, pp. 4567-4574, Nov.-Dec. 2015.

[19] I. Jeong, B. G. Gu, J. Kim, K. Nam and Y. Kim, "Inductance Estimation of Electrically Excited Synchronous Motor via Polynomial Approximations by Least Square Method," in *IEEE Transactions on Industry Applications*, vol. 51, no. 2, pp. 1526-1537, March-April 2015.